

# PERFORMANCE OF THE ESS HIGH ENERGY BEAM TRANSPORT UNDER NON-NOMINAL CONDITIONS

H.D. Thomsen\*, S.P. Møller, ISA, Aarhus University, 8000 Aarhus C, Denmark

## Abstract

With a nominal beam power of 5 MW, the demands for low relative beam losses in the European Spallation Source (ESS) accelerator are unprecedented. In the High Energy Beam Transport (HEBT), where the beam first reaches full power, this is especially relevant. The acceptance of the HEBT should thus encompass beams of non-nominal parameters and ideally be tolerant to partial hardware failure for at least a pulse train of 2.86 ms. In this paper, the sensitivity towards errors in beam parameters and optical elements will be presented.

## INTRODUCTION

The nominal HEBT optics is described in [1] and there shown to efficiently transport the intense proton beam from the linac to the spallation target. Lattice and beam imperfections will however exist in any realistic accelerator and could potentially augment primary beam losses. The transport line should thus either provide means to measure and neutralize an error or be built with tolerances that minimizes the impact to a tolerable level. An error and sensitivity analysis will help to assess *e.g.* mechanical alignment and stability tolerances.

A wide range of typical sources of errors affecting the beam will be analyzed in the following. The errors are classified into two different kinds: dynamic (fast) and static (slow). The dynamic errors have an origin or change on a timescale that generally prevents feasible correction schemes. This could be magnet support vibrations (displacements) or ripple from the magnet power supply. Static errors can on the contrary be corrected by detecting a semi-constant beam parameter displacement, *e.g.* a beam orbit excursion resulting from a transversely displaced quadrupole. Contrary to the name, static errors may have a time-dependence, *e.g.* localized foundation settlement, albeit very slow (months or years). Using a combination of dipole correctors (steerers) and downstream beam position monitors (BPMs), it is in theory straightforward to correct for static magnet displacements and beam displacements (spatial or angular). An error-correction analysis can however still be helpful in terms of optimizing the quantity and locations of correctors and the associated beam instrumentation. Besides tightening tolerances on relevant equipment (more stable magnet power supply, magnet support, etc.), there are no means to correct for dynamic errors. Studies of dynamic errors can however help to design a nominal beam lattice, where the impact of sudden or dynamic errors are minimized at critical locations, *e.g.* the spallation target front face, the beam entrance window (BEW).

\* heinetho@phys.au.dk

Table 1: Definition of Error Types and Magnitudes. Unless otherwise specified, the values represent the half-width of a uniform distribution centered around 0

Element	Parameter	Unit	Static	Dynamic
Quadrupole	$dx, dy$	mm	0.2	0.01
	$d\hat{z}$	deg	0.03	0.003
	Gradient	%	0.5	0.02
Dipole	$dx, dy$	mm	0.2	0.01
	$d\hat{z}$	deg	0.03	0.003
	Strength	%	—	0.02
Beam	$dx, dy$	mm	2	0.25
	$dx', dy'$	mrad	0.1	0.01
	Energy	MeV	20	2.5
	Emittance	%	10	1
	Mismatch	%	10	1
	Current	mA	1	0.1

Transporting the beam to the target, the HEBT consists of a long transport section (the UHB), a vertical dogleg, and finally the A2T, interfacing to the target monolith [1]. Apart from in the A2T, all quadrupoles have auxiliary coils to introduce a steerer field acting in the focusing plane only. A UHB/dogleg doublet thus contains a steerer in each transverse plane.

As part of the raster beam expander system intended to reduce the beam intensity on the proton beam window (PBW) and target, the final part of the A2T contains a strong quadrupole doublet before a  $\approx 21$  m flight tube to the target. This combination may excessively magnify dynamic errors and consequently set very strict dynamic tolerances on the final beam elements. The A2T contains 4 combined horizontal and vertical steerer units with the aim of neutralizing the beam displacement and angle just before the raster magnets and before the target flight tube. It should be noted that the studies presented here are based solely on the DC optics, *i.e.* having the AC raster magnet system off.

## PROCEDURE

The error types and magnitudes can be seen in Table 1. These are implemented in TraceWin [2], which is used for the simulations. Included are magnet transverse displacement ( $dx, dy$ ), roll  $d\hat{z}$ , and strength offset. The two dipoles are powered by a single power supply, hence the dipole strength errors are introduced as a coupled error. All other errors are treated as uncoupled. Besides phase space displacements ( $dx, dx', dy, dy'$ ), the HEBT input beam is exposed to energy jitter, emittance and current increase. A mismatch factor  $m_w$  also affects the Twiss parameters,

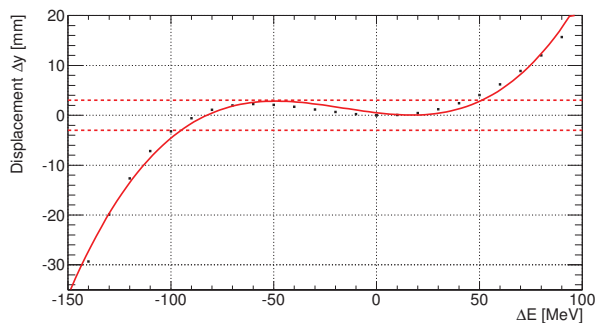


Figure 1: The beam's vertical displacement on the target front face (BEW) as a function of  $\Delta E$ .

$(\alpha_w, \beta_w) \rightarrow (1 + m_w) \times (\alpha_w, \beta_w)$  in each plane  $w = x, y, z$ . The magnitudes of the errors have been set by looking at similar single-pass lines but also by consulting experienced magnet designers. For reference the RMS beam size is  $\approx 2$  mm.

## ENVELOPE STUDIES

When including dipoles in a transfer line, the behaviour of off-momentum beam is essential to study. As a result of RF failures along the linac, which can occur on an ultra-fast timescale ( $\approx \mu\text{s}$ ), the beam may reach the HEBT with a significantly reduced energy,  $2.0 \text{ GeV} + \Delta E$ . Leaving no time to readjust the downstream magnets, the dominant effect will be a vertical displacement in the dispersive sections, *i.e.* the dogleg. Here, a maximum dispersion of  $D_y \lesssim 0.88 \text{ m}$  gives rise to vertical beam centroid displacements of  $\Delta y = (1 + 1/\gamma)^{-1} D_y \Delta E/E \approx 0.33 \text{ mm/MeV}$  ( $E = 2.0 \text{ GeV}$  assumed). At  $\Delta E = 75 \text{ MeV}$ , the maximum displacement in the dogleg is about 25 mm, effectively reducing the 50 mm aperture radius by a factor 2. Dynamic energy errors (jitter) are expected to be about 30 times smaller in magnitude, *i.e.*  $\Delta y \lesssim 0.8 \text{ mm}$  at maximum  $D_y$ , which should only just be detectable.

It should be noted that the dogleg is only a linear achromat, meaning that higher-order dispersion can prevail downstream of the dogleg. The impact of beam energy jitter and sudden energy deficits on the stability of the beam at the target is thus also relevant. In Fig. 1, the vertical beam displacement at the target is seen as a function of the HEBT input beam energy while keeping all other settings constant. The dispersive effect is clearly dominated by quadratic and cubic terms. From this plot, the correlation between energy jitter and vertical BEW displacement can be seen directly. A cubic fit is shown along with the data points. The dashed lines in Fig. 1 mark the max. displacement requirement ( $|\Delta y| < 3 \text{ mm}$ ), which is seen to be met for a very wide energy interval,  $-100 \text{ MeV} \rightarrow +50 \text{ MeV}$ .

Initial studies show that apart from beam energy errors, the BEW beam parameters are in general most sensitive to the applied errors, due to the above mentioned magnification. To quantify the impact of the various error types, the

beam centroid displacement ( $\Delta w, w = x, y$ ) and RMS size ( $\sigma_w$ ) is thus simulated at this location using envelope calculations and introducing errors. In both cases, the results are scaled by the horizontal and vertical nominal beam sizes, 15.9 mm and 5.3 mm, respectively. For each error group, and also the total of all groups combined, 1000 HEBTs (*i.e.* sampling the stochastic errors) are simulated. The impact of the dynamic errors are seen in Fig. 2, left panels. The quadrupole and beam parameter errors contribute equally to the displacement, while the latter is the dominant source of changes in beam size. The effects of the implemented dynamic dipole errors are minute, partly due to the coupling through a single power supply. In general, the absolute dynamic impacts are small and largest in the horizontal plane,  $\text{RMS}(\Delta x) = 2.4 \text{ mm}$  and  $\text{RMS}(\sigma_x) \lesssim 0.2 \text{ mm}$ . The assumed dynamic parameters, *e.g.* 200 ppm magnet strength stability, appear to be tolerable.

Similarly, the uncorrected static errors are simulated, initially without applying any compensating corrections, *cf.* Fig. 2, middle panels. Clearly the uncompensated static errors have an unacceptably large impact on the beam displacements (notice the larger scales),  $\text{RMS}(\Delta x) = 36 \text{ mm}$ . This is largely due to the quadrupole misalignments,  $dx, dy$ , inducing unintended beam deflections. The beam size is also affected and a maximum of 40% horizontal beam size increase is found.

## Correction Strategy

A set of correction methods is implemented to compensate for the static errors. The HEBT line contains numerous BPMs and steerers, either embedded in the primary dipoles or quadrupoles (UHB + dogleg) or as separate elements (A2T). The accuracy of the beam position measurement close to the A2T magnets and close to the target are assumed to be 1 mm and 2 mm, respectively. As a test of the section's flexibility, the beam size is in this study corrected using only the A2T quadrupoles, although the HEBT line contains a large number of independent quadrupoles. By adjusting these 6 quadrupoles, the beam size is corrected at two critical locations, the target and the raster magnet action point [1]. In the nominal optics there is a direct relation between the beam size at the action point and that at the HEBT's minimum physical aperture, a  $\text{Ø}40 \text{ mm} \times 2000 \text{ mm}$  neutron shield wall (NSW) between the final magnets and the target. This relation is exploited to indirectly measure and set the beam size at the NSW center. The efficiency of relying on this principle is interesting to study when subjecting the line to errors, *cf.* below.

Envelope simulations of static errors including corrections can be seen in Fig. 2, right panels. The displacement distributions are clearly characterized by the  $\pm 2$  positioning accuracy at the target, which has successfully been met in all the simulated lines. To reach this goal, some of the steerers embedded in quadrupoles have a maximum strength of 3.5 mT.m, while the separate A2T steerer units reach 15 mT.m. The beam size distribution is very narrow with  $\lesssim 5\%$  change.

Content from this work may be used under the terms of the CC BY 3.0 licence (© 2014). Any distribution of this work must maintain attribution to the author(s), title of the work, publisher, and DOI.

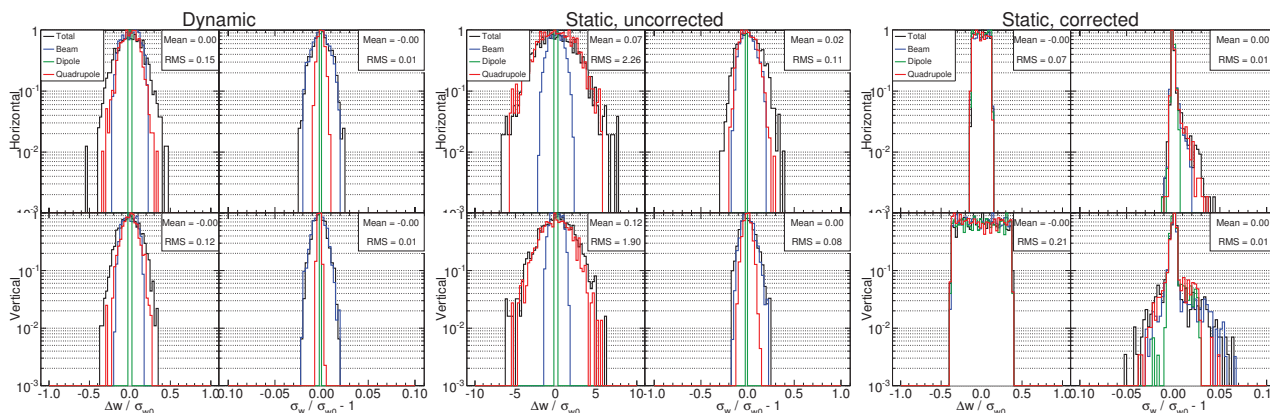


Figure 2: Simulations of the beam parameter changes at the BEW when subjected to the different error categories and magnitudes. The mean and RMS are calculated for the total simulation. All distribution amplitudes are normalized to unity. Notice the different horizontal scales.

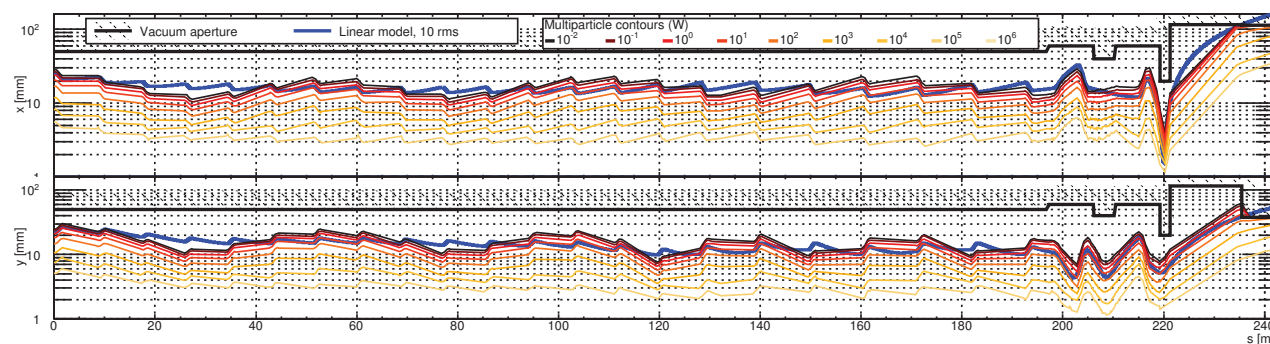


Figure 3: Multiparticle simulations including dynamic and corrected static errors.

## MULTIPARTICLE STUDIES

Combining all of the above, an error study based on multiparticle simulations is performed. Specifically, the envelope optics are used to apply dynamic and static errors and correct the latter using a range of virtual diagnostics. For each of 1000 simulated HEBTs, the achieved optics is then the basis of a multiparticle simulation with  $10^6$  macroparticles. The applied input beam distribution consists of two overlapping Gaussians: a primary (99%) Gaussian distribution and a secondary (1%), with  $5\times$  emittance, representing beam halo. The simulated HEBTs have been combined and are represented in Fig. 3 by contour lines that transversely enclose beam power levels. The contours are to a large extent comparable to the 10 RMS nominal beam size envelope (blue line). Due to the uncorrected input beam mismatch, some beta-beating is visible in the first 200 m. This is also believed to be the cause of an observed increase in transverse emittance, typically 10%, max. 20%, within the first 50 m of the HEBT. This could be reduced by applying the corrective matching in the beginning of the HEBT.

Low intensity losses (on average 11 W, max. 100 W) are observed at the target monolith edge ( $s \approx 236$  m) with typically 0.6 kW, max. 1.4 kW, hitting the inner walls of the

monolith beam duct leading to the target. The loss magnitudes are not considered critical, and it should be noted that this can be reduced by adjusting the beamlet dimensions. It is very comforting to see that the simulations indicate that the beam waist at the NSW aperture ( $s \approx 220$  m) can be preserved despite applying the errors.

## CONCLUSION

Simulations of dynamic and static imperfections of the HEBT beam and lattice have been performed using input error magnitudes that are believed to be realistic for a single-pass transport line from a linac. The introduced dynamic effects have a modest impact on the beam. In general, the correction schemes appear to be able to restore the beam parameters to an acceptable degree. It should be noted that the simulated primary beam losses can depend very much on the input distribution. To properly quantify the levels is left for a more detailed study.

## REFERENCES

- [1] H.D. Thomsen *et al.*, IPAC'14, WEPRO073 (2014).
- [2] R. Duperrier *et al.*, ICCS'02, LNCS2331, p. 411 (2002).